

# **Inclusion Models of Laser Damage**

**Jeffrey Wilbur**

**Victor Senior High School**

**LLE Advisor: Prof. John C. Lambropoulos**

**Summer 2001**

## **ABSTRACT**

Inclusion models of laser damage were constructed using Mathematica v. 4.0. These models predict the effect of the inclusion interface on the damage threshold, by comparing inclusions with perfect and totally imperfect interfaces. The perfect interface models were based on the Goldenberg and Tranter heat conduction solution. With these models, the effects of variables such as pulse length and inclusion radius could be studied. An equation for the totally imperfect interface was then developed using relationships between these variables, and by taking into account that no heat conduction occurs between this interface and the surrounding matrix. With these models, scaling of the damage threshold was developed, and the models showed the effects of the different initial interfaces.

## **1. OVERVIEW**

### **1.1 Introduction**

Today, the study of laser damage is one of the most important and rapidly advancing fields in all of laser physics. This field of study investigates all aspects of damage in the laser system, ranging from physical damage on the laser, the lens, and the target, to the theoretical study of why this damage is occurring. This research is instrumental in the future of laser physics, and it is these various lens defects which are becoming a prominent obstacle in the creation of an efficient and practical laser-based system. The damage caused by lens defects is extremely costly, and prevents the laser system from working to its full potential. If this damage can be prevented, thousands of dollars can be saved, and the laser systems will be more efficient and productive.

### **1.2 Outline**

To work with the theoretical aspect of why laser damage occurs in the optics of the laser, it was necessary to create computational models that duplicated the physical properties of the laser lens. To develop these models, programs were created and conditions were simulated using

Mathematica v. 4.0. With the assistance of this program, the necessary calculations could be constructed and organized.

In order to correctly duplicate the physical properties of the lens, its material properties, as well as those of the defect, were examined. The material properties that were investigated mainly dealt with the properties of the absorbing inclusion, which were density, specific heat, thermal conductivity, and thermal diffusivity. Since these properties vary according to the composition of the defect, the calculations were performed using values from the most common types of inclusions.

After reviewing the physical properties of the absorbing inclusion, it was also necessary to consider the thermal interaction (heat conduction and heat flux) between the defect and the surrounding lens matrix. To examine this interaction, the investigation of the interface between these two materials was crucial. The two interface models used for these calculations were the perfect and totally imperfect interfaces. These types of interfaces are the extreme possibilities, and although they rarely occur, they provide the limits to a range of simulations in which all other interfaces are included.

After taking into account many of the possible variables that influence laser damage, the computational models could be run. These models were created using the laws of thermodynamics and the heat conduction equation, as well as the Goldenberg and Tranter solution (when looking at the perfect interface model). Through experimentation and simulation of different combinations of variables, I studied the effect of the radius of the inclusion on the damage threshold of the inclusion: it was determined that a specific combination of variables produced a worst case scenario. In this scenario, the lens was most prone to melting and damage. After this situation was examined, the effect of the individual variables was also determined, and a scaling of damage threshold for both the perfect and totally imperfect interface was constructed.

## **2. DEVELOPMENT OF INCLUSION MODELS**

### **2.1 Absorbing Inclusion Inside Non-Absorbing Matrix**

In order to set up the theoretical calculations in Mathematica, the physical properties of an inclusion model had to be duplicated. The model that was simulated was an absorbing spherical inclusion embedded inside a non-absorbing infinite matrix. In this model, the defect is located inside the non-absorbing lens. This is important because as the laser light is passed through the lens, the inclusion is the only material that will absorb any of the energy from the laser. The other light passing through the lens matrix is not absorbed, and does not have any effect on the system.

When programming this model into Mathematica, it was also necessary to make assumptions about the properties of defect, the interface, the matrix, heat flux, the laser pulse,

and the rise time of the laser. These assumptions simplified the calculations so that a general model could be used for all of the calculations. The first assumption that was made concerned the idea of how the inclusion absorbed energy from the laser. In this model, it was assumed that the energy absorbed by the inclusion was equal to the laser's energy flux ( $J/m^2$ ) multiplied by the inclusion cross sectional area ( $\pi R^2$  for a spherical inclusion of radius R.) There were also assumptions regarding the point at which damage actually occurs. In this model, it was assumed that damage occurs when the temperature at the center of the inclusion is equal to the inclusion's melting point.

The assumptions regarding the interface dealt with the difference between the perfect and imperfect interface. For the perfect interface, it was assumed that this interface allowed for complete heat conduction between the inclusion and the surrounding matrix. The opposite was assumed for the totally imperfect interface. In this interface, it was assumed that the interface was so insulating that it did not allow for any heat conduction or energy flow between the two materials. The shape and rise time of the laser pulse were also assumed. For this model, it was assumed that there was no rise time for the laser, meaning that as soon as the laser was activated, the beam was at its maximum power. Although these two assumptions are not very practical, because the laser pulse generally does have a curved shape with a rise time, they were used to develop the general model. The last assumption that was used in the creation of this inclusion model was that heat absorption is instantaneous and uniform over the inclusion. This was done to assure that the whole defect was affected by the laser energy, and that absorption was uniform across the whole inclusion.

The assumptions are summarized as follows:

Spherical inclusion;

Inclusion absorbs energy =  $(E \pi R^2)$ ;

Damage occurs when  $T_{\text{center}} = T_{\text{mp}}$ ;

Perfect interface: Complete heat conduction across interface;

Totally imperfect interface: No heat conduction across interface;

Laser: Square pulse shape and no rise time;

Instantaneous and uniform heat absorption.

## 2.2 Interface Equations

After the physical properties of the inclusion model had been created, the Mathematica v. 4.0 equations had to be designed and programmed. For these equations, the problem was divided into two different sections. One section deals with the perfect interface, and the other dealing with the totally imperfect interface. Each of these interface models needed a different equation because they each had different physical properties. For the perfect interface scenario, the Mathematica program could be based on the Goldenberg and Tranter solution [1952]. This

equation was used because it considered the effects of heat conduction across the perfect interface, and it allowed for the comparison between the damage threshold and the size of the inclusion. See Appendix 1 for a copy of the Mathematica v. 4.0 program [Wolfram, 1996].

The Goldenberg Tranter result for the perfectly conducting interface is

$$T_{\text{center}} = (R^2 A / k_1) F[k_1/k_2, tp D_1/R^2, (\rho_1 C_1)/(\rho_2 C_2)] \quad (1)$$

Here subscript 1 denotes the inclusion, and subscript 2 the matrix.  $k$  is thermal conductivity (W/m.K),  $D$  is thermal diffusivity (m<sup>2</sup>/s),  $tp$  is pulse duration,  $R$  is the inclusion radius,  $\rho$  is mass density (kg/m<sup>3</sup>), and  $C$  is heat capacity (J/kg.K). The quantity  $A$  (units W/m<sup>3</sup>) is power absorbed per unit volume in the inclusion, and found from the absorbed energy ( $E \pi R^2$ ) divided by the pulse duration ( $t$ ) and the inclusion volume ( $4 \pi R^3/3$ ). The form of the function  $F$  can be found in Goldenberg and Tranter [1952].

For the totally imperfect interface scenario, a new equation had to be created. In order to develop this formula, it was necessary to review the equation relating energy absorbed  $Q$  and temperature change  $\Delta T$  in a body of mass  $m$  and specific heat  $C$ :

$$Q = m C \Delta T \quad (2)$$

In order to manipulate this into a useable formula, it was necessary to substitute in for the mass  $m$ . Since mass is equal to density  $\rho$  multiplied by volume  $V$ , those new equations could be inserted instead in place of the mass:

$$E \pi R^2 = \rho V C \Delta T, \text{ or}$$

$$(E \pi R^2) = \rho (4/3 \pi R^3) C \Delta T \quad (3)$$

This formula could then be solved for the temperature change  $\Delta T$  and manipulated into a form that could be programmed into Mathematica. The result for the temperature rise at the center of inclusion with the totally imperfect interface equation is

$$T_{\text{center}} = 3E / [4R * (\rho C)] \quad (4)$$

## 2.2 Material Properties

After the perfect and totally imperfect interface equations had been programmed in Mathematica, their variables needed to be researched and examined. The variables that needed to be researched for the two equations were density, specific heat (at both room temperature of

three hundred degrees K and one thousand degrees K), and thermal conductivity (at both three hundred degrees K and one thousand degrees K). In order for this data to be relevant, these properties were recorded for thirteen different, but common defect materials. After recording all the values, it was then possible to further investigate the properties of these variables. For each defect material, both  $(\rho C)$  and thermal diffusivity ( $D = k / (\rho C)$ ) were calculated and their values were compared for all the materials, see Appendix 2.

The interesting fact that was discovered from this comparison was that while the density, thermal conductivity, and thermal diffusivity differed greatly among the various materials, the value of  $(\rho C)$  remained approximately constant. This was an important discovery which allowed the interface equations to be simplified by removing the variable  $(\rho C)$ . Since the  $(\rho C)$  value was approximately constant for all defect materials, it would not have any distinct influence in the damage threshold calculations.

### 3. CALCULATION RESULTS

#### 3.1 Procedure

The object of the interface calculations was to determine if a minimum radius  $R_{\min}$  existed, and if it caused a minimum damage threshold  $E_{\min}$ . In order to answer these questions, it was necessary to perform many calculations using the interface equations programmed into Mathematica. For each calculation, one variable was changed to determine how it affected both the  $R_{\min}$  and  $E_{\min}$  values. For each test, it was also necessary to determine the smallest  $R_{\min}$  value in order to calculate an accurate damage threshold value. While one variable was being tested, all others were kept constant to ensure that the calculations illustrated only the effects of one variable. After completing the calculations for the variable, the results were graphed and analyzed. The different variables tested were thermal conductivity of the inclusion ( $k_1$ ), thermal conductivity of the matrix ( $k_2$ ), thermal diffusivity of the inclusion ( $D_1$ ), time pulse of the laser ( $tp$ ), and the melting point of the inclusion ( $T_{mp}$ ),

#### 3.2 Perfect Interface Results

The first calculations that were done with the perfect interface equation revolved around determining the damage threshold of the inclusion. In these calculations, the initial goal was to compare the size of the inclusion to the damage threshold at that point. In these damage threshold calculations, the radius size  $R$  varied from  $0.1 \times 10^{-6}$  meters ( $0.1 \mu\text{m}$ ) to  $3 \times 10^{-6}$  meters ( $3 \mu\text{m}$ ).

After these results were graphed, an interesting fact was revealed, see Fig. 1. The graphs showed that there was a specific defect size ( $R_{\min}$ ) that caused the damage threshold to be at its lowest point ( $E_{\min}$ ). This showed that there was a worst defect size where the lens was most prone to damage. This calculation was then recreated using various pulse times  $tp$ , from  $1 \times 10^{-9}$

seconds to  $50 \times 10^{-9}$  seconds. These calculations also showed that the worst defect size existed at all the various time pulse lengths, although both the  $R_{\min}$  and  $E_{\text{cmin}}$  values changed at the different time pulse values  $t_p$ .

After comparing how the time pulse influenced the  $R_{\min}$  and  $E_{\text{cmin}}$  values, it was time to calculate the effects of the other variables: thermal conductivity of both the inclusion and matrix, ( $\rho C$ ), thermal diffusivity of the inclusion, and the melting point of the inclusion. In these calculations, both the  $R_{\min}$  and  $E_{\text{cmin}}$  values were calculated while observing the effects of the other variables.

After repeating the damage threshold calculations with the inclusion's melting point as the variable, it was observed that the  $E_{\text{cmin}}$  varied proportionally to melting point, see Fig. 2, while the melting point had no effect on the value of  $R_{\min}$ , see Fig. 3.

After repeating the damage threshold and minimum radius calculations with the time pulse of the laser as the variable, it was observed that both  $E_{\text{cmin}}$  and  $R_{\min}$  varied proportionally to the square root of the time pulse  $t_p$ . See Figures 4 and 5.

Then, the damage threshold and minimum radius calculations were repeated using first, the thermal conductivity of the matrix as the variable, and then, using ( $\rho C$ ) as the variable. With the thermal conductivity as the variable, it was observed that both  $E_{\text{cmin}}$  and  $R_{\min}$  varied proportionally to the square root of the thermal conductivity. With ( $\rho C$ ) as the variable, it was observed that  $E_{\text{cmin}}$  also varied proportionally to the square root of ( $\rho C$ ), see Fig. 6, but  $R_{\min}$  varied proportionally to the negative square root of ( $\rho C$ ), see Fig. 7.

### 3.3 Scaling of $E_{\text{cmin}}$ and $R_{\min}$

After observing the results from the perfect interface calculations, the relationships between the different variables (thermal conductivity, time pulse, melting point, ( $\rho C$ ), and both  $E_{\text{cmin}}$  and  $R_{\min}$  were revealed. By examining how each individual variable affected the damage threshold and minimum radius, two scaling equations were developed. These equations demonstrated the effects of the variables, and they helped to explain their relationship.

For the  $E_{\text{cmin}}$  scaling equation, each variable relationship was taken into account and examined. The calculations demonstrated that  $E_{\text{cmin}}$  varied as the square root of the time pulse, ( $\rho C$ ), and the thermal conductivity of the matrix, while varying proportionally to the melting point. Taking this data into account, and by matching the correct units, the  $E_{\text{cmin}}$  scaling equation was developed.

$$E_{\text{cmin}} = T_{\text{mp}} [t_p k_2 (\rho C)]^{1/2} f(k_1 / k_2) \quad (5)$$

with  $f$  a dimensionless function, see Fig. 8.

For the  $R_{\min}$  scaling equation each variable relationship was taken into account and examined. The calculations demonstrated that  $R_{\min}$  varied as the square root of the time pulse and the thermal conductivity of the matrix, but it varied as the negative square root of  $(\rho C)$ . They also showed that the melting point of the equation had no effect on the value of  $R_{\min}$ . Taking this data into account, and by matching the correct units, the  $R_{\min}$  scaling equation was developed.

$$R_{\min} = [tp \ k_2 * (\rho C)]^{1/2} \ g(k_1 / k_2) \quad (6)$$

Here, again,  $g$  is a dimensionless function, see Fig. 9.

### 3.4 Totally Imperfect Interface Results

For the totally imperfect interface calculations, the major objective was to determine the relationship between size of the inclusion and the inclusion's damage threshold. In order to find this relationship, it was necessary to use the imperfect interface equation that had been programmed into Mathematica. Since there was no heat flux or conduction across the totally imperfect interface, the calculation was much simpler. With thermal conductivity and diffusivity removed from the equation,  $E_{\text{cmin}}$  was now proportional to the inclusion size  $R_{\min}$ . These calculations also showed that the damage threshold was not affected by the time pulse  $tp$  of the laser. These results are shown schematically in Fig. 10. In this scenario, the data shows that there is not an inclusion size that is most prone to damage, and only the melting point of the inclusion will determine how predisposed the inclusion site is to melting.

## 4. CONCLUSIONS

After reviewing the results of both the damage threshold and inclusion size calculations, the relationships of the different variables was established. These relationships were displayed in both the  $E_{\text{cmin}}$  and  $R_{\min}$  scaling equations, and they helped to guide both the perfect and totally imperfect interface models. From these damage threshold calculations, it was determined that with the imperfect interface, the damage threshold was proportional to the radius of the inclusion multiplied by the time pulse of the laser. Although this information is very useful, the most important conclusion that can be drawn from these calculations is the idea that with a perfect interface, a worst defect size exists. At this worst size radius size, the damage threshold of the inclusion is at its lowest value, creating a situation where the inclusion is most prone to melting and damage. In these specific calculations, the worst defect size ranged from 40 to 300 nm, but this range is dependent on the material properties of the inclusion.

This idea of a worst defect size is very important to controlling the problem of laser lens damage. Knowing that a worst defect size will cause the most damage, it is important to look at

how to prevent the creation of this size defect. Since there is no way to control many of the natural inclusions that form in lenses, it is important to prevent inadvertent defects. When the lens is polished or coated, the size of the polishing abrasive slurry must be examined. Since polishing leaves some inadvertent defects in the lens, it is necessary to be sure these defects are not of the worst size. By first examining the size range of the worst defect, it would then be possible to use a polishing method that is less likely to cause this size defect. The polishing would still leave some inadvertent defects, but they would not be the size which is most prone to damage.

## **5. SUGGESTIONS FOR FURTHER WORK**

To further investigate how these calculations simulate the physical process of laser damage, it would be important to examine the effect of the laser's pulse shape and rise time. In our calculations, it was assumed that the laser had a square pulse shape and no rise time. In actuality, the laser does have a curved pulse shape and a rise time. In future work, to make these calculations more realistic, it might be important to investigate how the laser's properties influence the damage threshold and minimum size of the inclusion.

Another area to look at for further work would be in the details of absorption and heat transfer. It might be worth looking into how different wavelengths of light are absorbed by the inclusion, and if any specific wavelength has a greater effect on the damage threshold calculation. When looking at the details of heat transfer, it would be important to examine heat flux. More investigation is needed to determine if heat flux is instantaneous, and how a delayed heat flux might change the damage threshold calculations.

## **REFERENCES**

- Cengel, Yunus A. *Heat Transfer: A Practical Approach*. New York: The McGraw-Hill Companies, (1998).
- Exarhos, Gregory J. *Laser-Induced Damage in Optical Materials: 1998*. New York: The International Society for Optical Engineering, 1999.
- Goldenberg H. and M. A. Tranter M. A., Heat flow in an infinite medium heated by a sphere, *British Journal of Applied Physics*, vol. 3, pp. 296-298, 1952.
- International Critical Tables of Numerical Data, Physics, Chemistry, and Technology*. The McGraw-Hill Companies: New York, 1993.
- Stephen Wolfram. *The Mathematica Book*. Illinois: Wolfram Media, 1996.
- Touloukian, Y.S. *Thermophysical Properties of Matter and Substances*. Amerind Publishing Co., Washington DC, 1974.
- Wolf, Jonathan S. *AP Physics B*. Barron's, 1995.

```
In[156]:- f[R_, D1_, k1_, k2_, tp_, y_] :=
  (
    (Exp[-((y^2 * tp) / (R^2 / D1))] / y) *
    (
      (Sin [y] - (y * Cos[y])) /
      (
        ((1 - (k2/k1)) * Sin[y] - (y * Cos[y]))^2 +
        ((k2/k1) * y^2 * Sin[y]^2)
      )
    )
  )
```

```
In[157]:- a[R_, D1_, k1_, k2_, tp_, ymax_] := NIntegrate[f[R, D1, k1, k2, tp, y],
  {y, 0, ymax}, MinRecursion -> 0, MaxRecursion -> 100000]
```

```
In[158]:- try[ymax_] := NIntegrate[f[.01*10^-6, 3.5*10^-6, 8, 1.38, 30*10^-9, y],
  {y, 0, ymax}, MinRecursion -> 0, MaxRecursion -> 100000]
```

```
In[154]:- try[1]
```

```
Out[154]= 0.306125
```

```
In[160]:- try[1.2]
```

```
Out[160]= 0.306125
```

```
In[161]:-
```

```
a[.01*10^-6, 3.5*10^-6, 8, 1.38, 30*10^-9, 1.2]
```

```
Out[161]= 0.306125
```

```
In[162]:-
```

```
b[k1_, tp_, Tmp_, R_] := ((4 * k1 * tp * Tmp) / (3 * R))
b[8, 30*10^-9, 2000, .01*10^-6]
```

```
Out[163]= 64000.
```

```
In[164]:- c[k1_, k2_, R_, D1_, tp_, ymax_] := (1 /
  ((1/3) * (k1/k2) + (1/6) - ((2/ Pi) * Sqrt[k2/k1] * a[R, D1, k1, k2, tp, ymax])))
```

```
In[165]:- c[8, 1.38, .01*10^-6, 3.5*10^-6, 30*10^-9, 1.2]
```

```
Out[165]= 0.495518
```

```
In[166]:- Ec[k1_, tp_, Tmp_, R_, k2_, D1_, ymax_] :=
  b[k1, tp, Tmp, R] * c[k1, k2, R, D1, tp, ymax]
```

```
In[170]:- Ec[8, 30*10^-9, 2000, .01*10^-6, 1.38, 3.5*10^-6, 1.2]
```

```
Out[170]= 31713.1
```

## Material Properties

	P	C @ 300 K	C @ 1000 K	K @ 300 K	K @ 1000 K	PC @ 300 K	D @ 300 K
Units	kg/m <sup>3</sup>	J/(kg * C)	J/(kg*C)	W/(m*C)	W/(m*C)	J/(m <sup>3</sup> * C)	m <sup>2</sup> / s
Au	19300	129	x	317	x	2.50E+06	0.0001268
Al2O3	3960	756	1176	50	10	3.00E+06	1.66667E-05
BeO	2980	1050	1890	275	50	3.10E+06	8.87097E-05
CaF2	3170	924	1092	9.5	4	2.90E+06	3.27586E-06
CaCO3	2940	840	840	3.5	1.5	2.50E+06	0.0000014
GaAs	5316	315	357	33	27.5	1.70E+06	1.94118E-05
HfO2	9680	294	378	1.75	1.75	2.80E+06	0.000000625
MgF2	3110	1008	1260	33	x	3.10E+06	1.06452E-05
MgO	3590	1050	1260	55	9	3.80E+06	1.44737E-05
Si	2320	735	840	140	312	1.70E+06	8.23529E-05
ThO2	10009	231	315	8	3.5	2.30E+06	3.47826E-06
TiO2	4100	420	588	25	3.5	1.70E+06	1.47059E-05
Y2O3	5010	420	630	0.95	1.6	2.10E+06	4.52381E-07
max/min	8.31	813	6	333.68	208	2.25	281

# Laser Damage Thresholds

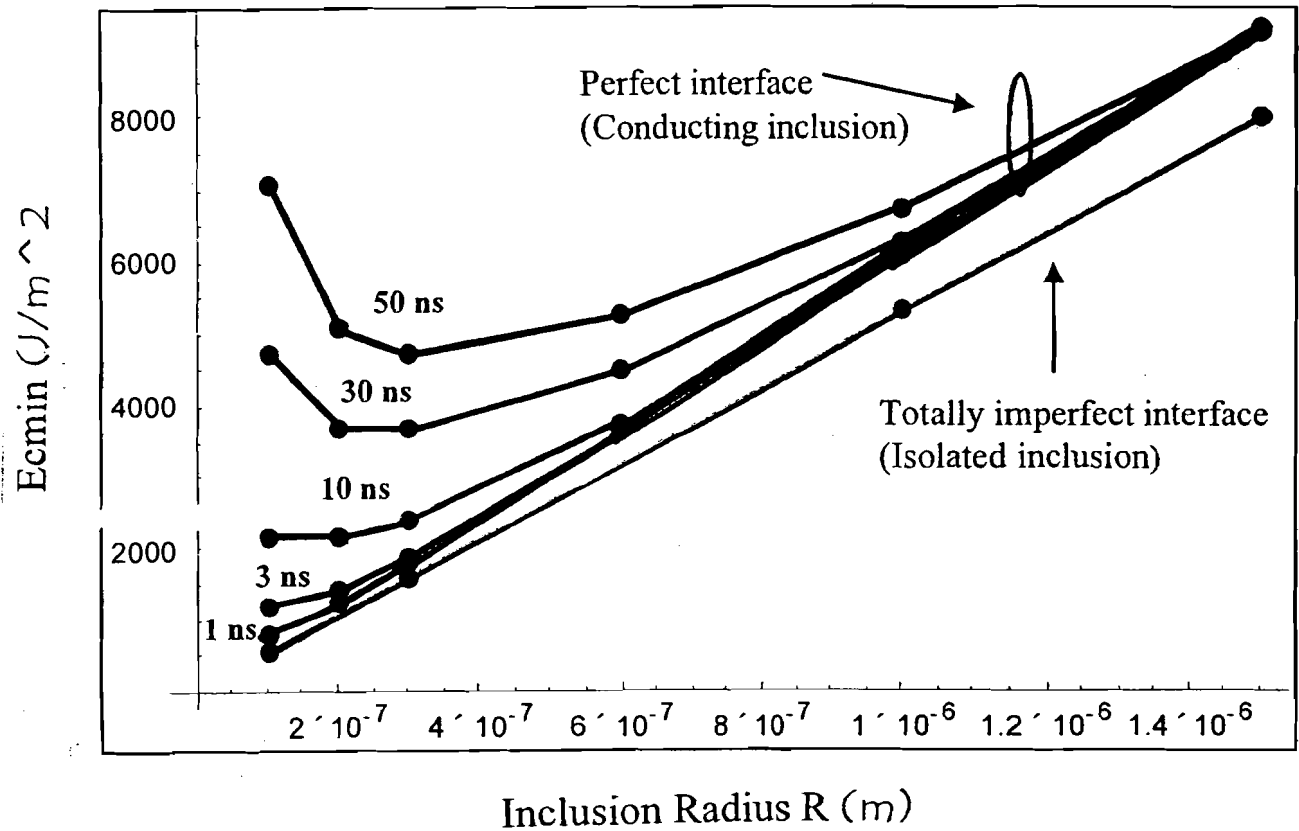


FIG. 1 The dependence of the laser damage threshold on inclusion radius  $R$  for various pulse durations  $t_p$ . The graph demonstrates the concept of minimum damage threshold. The graph also shows the result for the insulated inclusion (case of totally imperfect interface.)

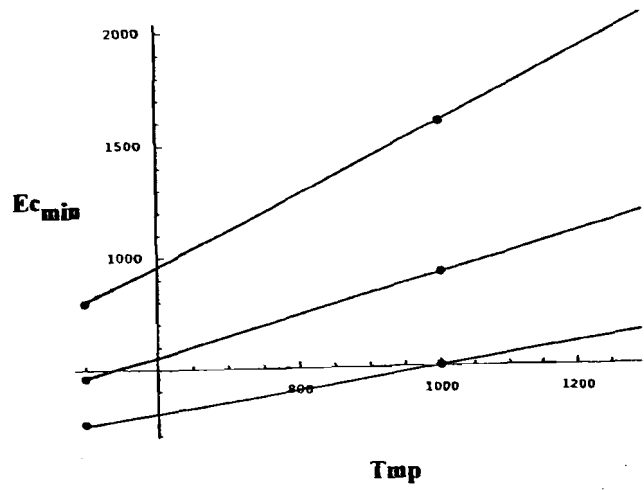


FIG. 2 Dependence of minimum laser damage threshold ( $J/m^2$ ) on the inclusion melting point (K).

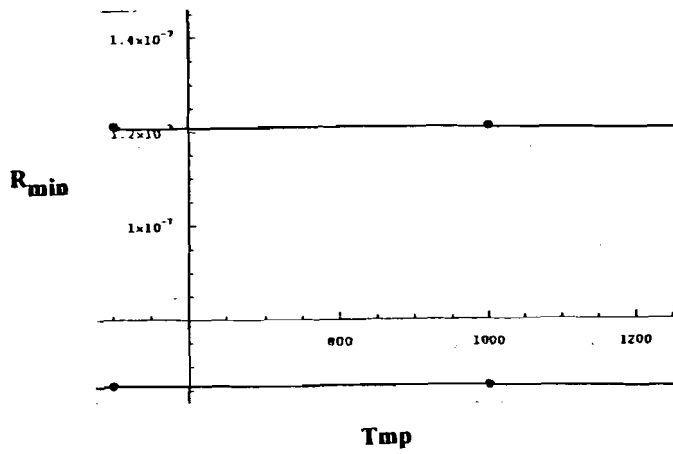


FIG. 3 Dependence of minimum inclusion size  $R_{min}$  ( $\mu m$ ) on inclusion melting point for two different pulse durations,  $t_p = 10$  ns (top) and  $t_p = 1$  ns.

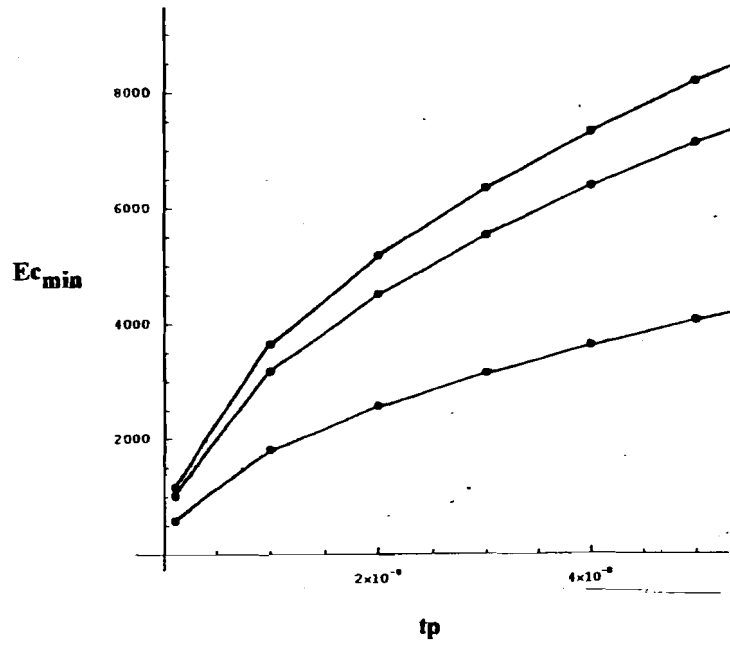


FIG. 4 Dependence of laser damage threshold ( $J/m^2$ ) on pulse duration (s).

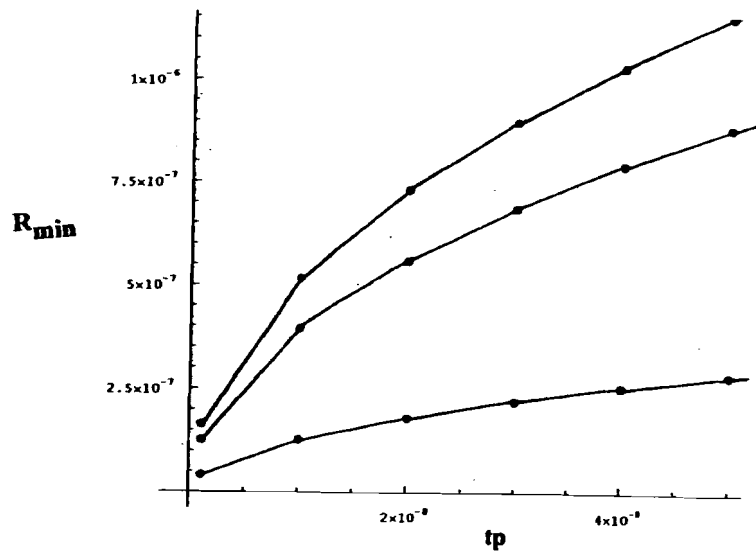


FIG. 5 Dependence of minimum inclusion size  $R_{\min}$  (worst defect radius, m) on pulse duration (s).

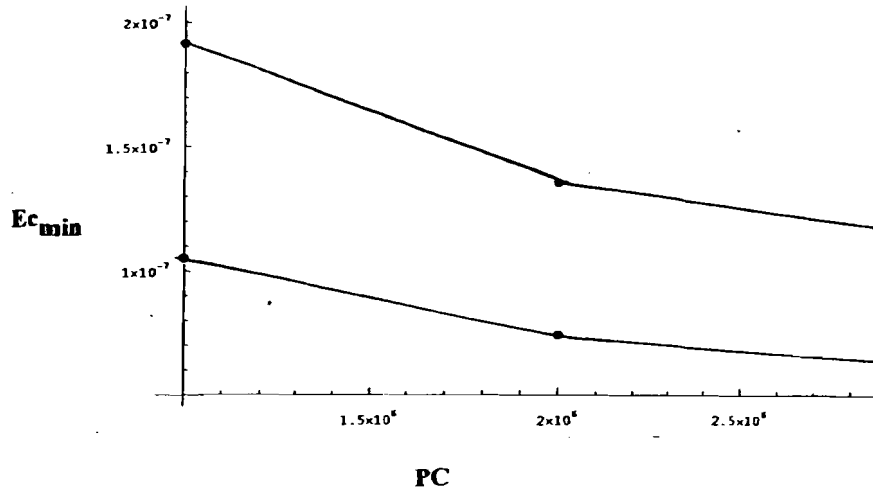


FIG. 6 Dependence of laser damage threshold ( $J/m^2$ ) on the product of mass density and heat capacity (product has units  $J/m^3.K$ ).

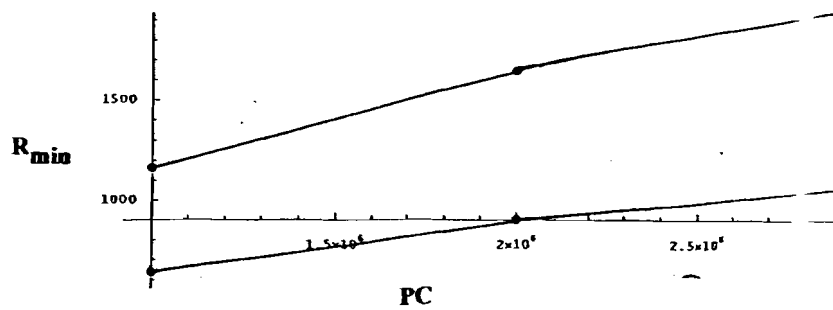


FIG. 7 Dependence of minimum inclusion size  $R_{min}$  (worst defect radius, m) on the product of mass density and heat capacity (product has units  $J/m^3.K$ ).

## SCALING: Minimum Areal Energy Density

---

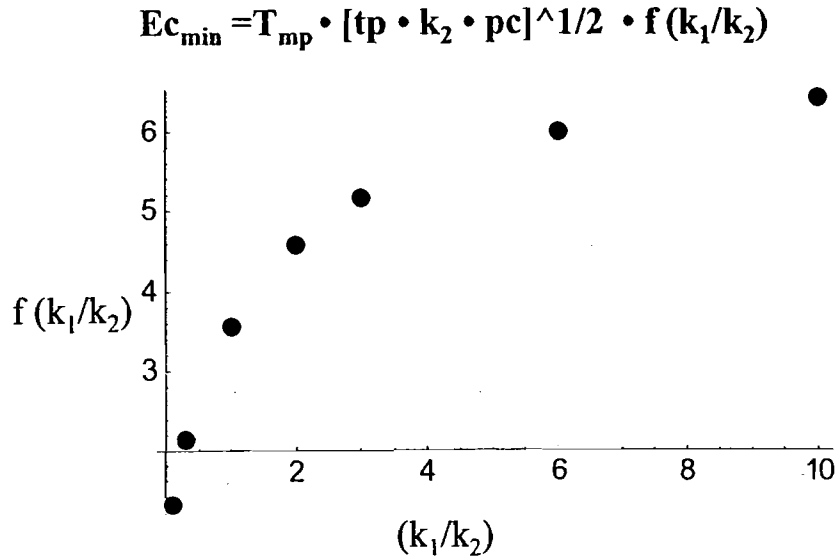


FIG. 8 Scaling of laser damage threshold  $E_{c_{\min}} = T_{mp} [tp \cdot k_2 (\rho C)]^{1/2} f(k_1/k_2)$  on pulse duration  $tp$  and thermophysical properties of the matrix and inclusion. The function  $f$  is dimensionless.

## SCALING: Worst Defect Size

---

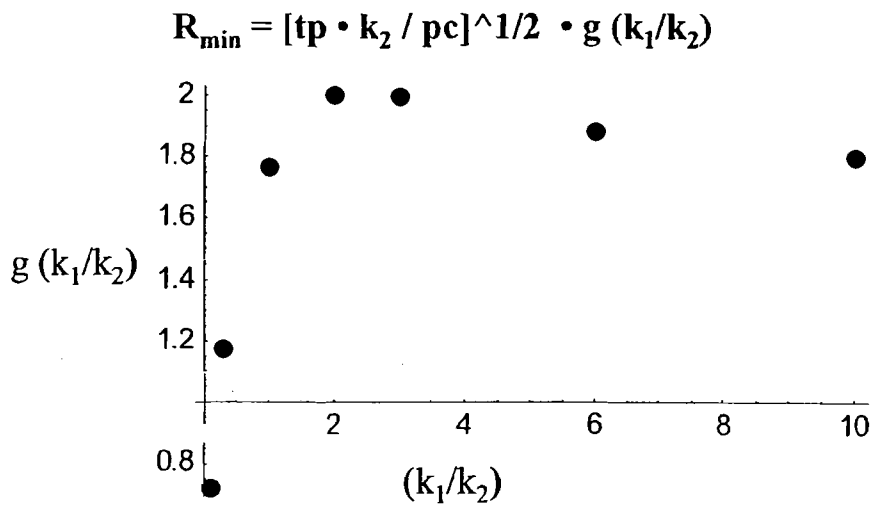


FIG. 9 Scaling of the minimum inclusion size  $R_{\min}$  (worst defect radius)  $R_{\min} = [tp \cdot k_2 \cdot (\rho C)]^{1/2} g(k_1/k_2)$ . The function  $g$  is dimensionless.

## Scaling: Effect of Interface

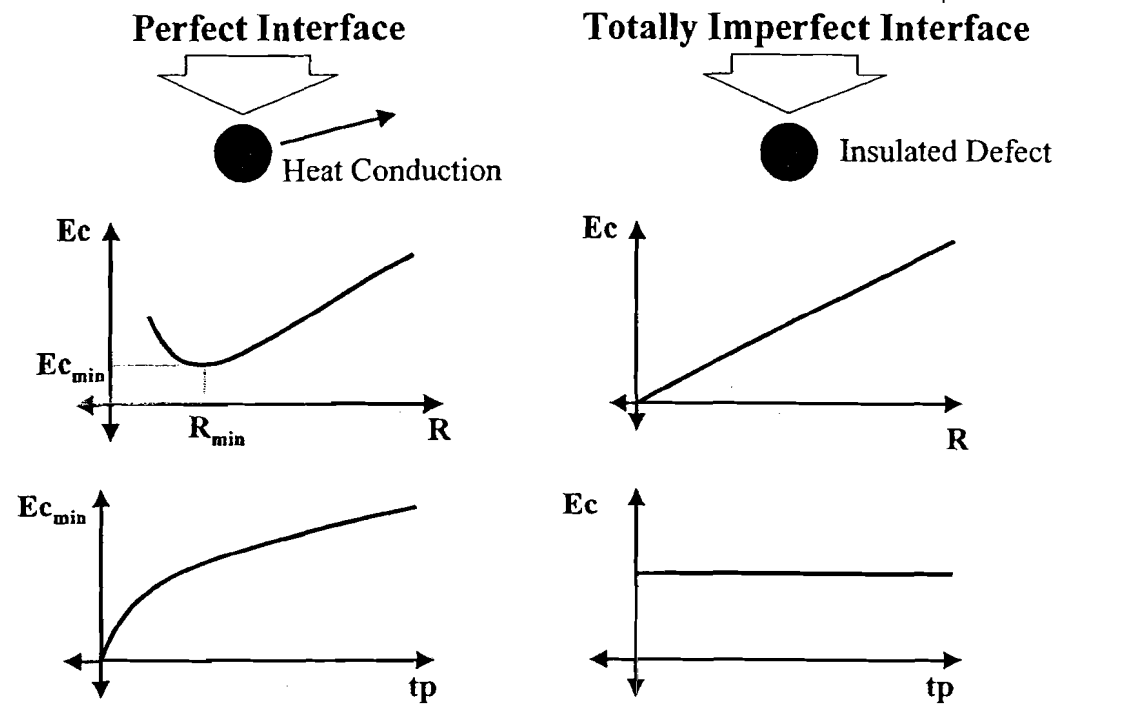


FIG. 10 Scaling of damage threshold ( $J/m^2$ ) on inclusion size and pulse duration for the case of the totally imperfect (insulating) inclusion.